Vibration Suppression Algorithms for NFIRAOS on TMT

C. Correia[a,*], J.-P. Véran[a], G. Herriot[a], B. Ellerbroek[b], L. Wang[b], L. Gilles[b]

[a]Herzberg Institute of Astrophysics, National Research Council, Canada
[b] Thirty Meter Telescope Observatory Corporation, Suite 200, 1111 S. Arroyo Parkway, Pasadena CA, USA
*carlos.correia@nrc.gc.ca

Abstract. Vibration suppression in Astronomical Adaptive Optics (AO) systems has gathered great attention in the context of next-generation instrumentation for current telescopes and future Extremely Large Telescopes (ELTs). This paper focus on the application of a novel multi-rate algorithm formulated in [Correia et al., 2011] to the 1st-light Multi-Conjugate Adaptive Optics Facility (NFIRAOS) for the Thirty-Meter Telescope (TMT). Numerical simulations cover the case of vibration peaks in the [2-225] Hz range with variable peak width based on telemetry from the Keck observatory. A comparison to other vibration suppression algorithms is performed using control loop framerates in the range [20–800] Hz, required to sense natural guide stars with magnitudes from $m_v \sim \{12 - 22\}$ in H-band.

1 Vibrations in AO systems

Vibrations, whether common or non-common path, affect most if not all the current operating Adaptive Optics (AO) systems, despite the efforts to either remove their sources or isolate them from the light paths. See [Clenet et al., 2004], [Veran and Poyneer, 2009], [Hess et al., 2003] and [Borelli et al., 2010] for the ESO-VLT, Gemini, Keck Observatories and LBT respectively. The problem with vibrations is even more critical for the proposed next generation of 20-40m Extremely Large Telescopes (ELTs) because the residual image jitter, particularly affected by vibrations, must be kept to within a small fraction of the diffraction limit, a mere few milliarcseconds (mas) RMS; the same applies to coronograph-based planet imagers on the current generation of 8-10m telescopes because the efficiency of most coronographs significantly drops if even the slightest image jitter is present.

Vibrations originate from a myriad of different sources: structural vibrations of the telescope and pre-focal mirrors due to wind buffeting, rigid body resonances, motor rotation, power ripples, cryogenic pumps, cooling fans and hydraulic bearing systems to list a few. Vibrations can directly affect the propagation of the science light, often by causing additional image jitter (tip-tilt). Vibrations can also perturb the operation of the AO system by corrupting the WFS path only, *i.e.* non common-path disturbances – causing the AO system to correct for disturbances that actually have no effect on the science path.

Moreover, vibrations often occur at frequencies near or beyond the AO bandwidth, and thus, may be poorly corrected. This results in excessive residual image jitter, which broadens the core of the point spread function (PSF), and reduces the Strehl-ratio.

1.1 Vibration suppression algorithms for laser-tomographic AO systems

Dedicated controllers specifically able to cancel out vibrations have been proposed in the context of the Very Large Telescope's SPHERE [Meimon et al., 2010] and the Gemini Planet Imager (GPI) instruments [Poyneer and Véran, 2010]. These use the Linear Quadratic Gaussian (LQG) framework under the implicit assumption that the AO sampling frequency is considerably higher than the vibrations' natural frequencies. While this assumption is generally true for planet finder type systems which always use a bright guide star and thus typically run at 1-2kHz sampling frequencies, it will not hold for laser-tomographic AO systems such as the ones envisioned at first light for ELTs. The reason is that, though these systems use laser guide stars (LGS), low-order modes as tip-tilt (TT) and

TT-anisoplanatism modes must be sensed on multiple natural guide stars (NGS). On top of this, sky-coverage requirements push the limiting magnitudes of the NGS to become even more fainter thus demanding greater integration times *i.e.* lower sampling frame rates. For example with NFIRAOS, the proposed first light AO instrument for TMT, the median AO frame rate for tip-tilt control is 90Hz [Wang et al., 2009] whereas the vibrations' natural frequencies are expected in the range [30–200] Hz (see e.g. [Veran and Poyneer, 2009]). When the AO sampling frequency is low compared to the vibration frequencies, the LQG-based methods previously proposed fail to provide an adequate level of rejection, thus calling for novel solutions.

1.2 Multi-rate algorithms

Laser-tomographic systems intrinsically use two frame rates: a higher one to the high-order LGS loop (and to drive the deformable mirrors) and a second one for the NGS modes where the vibrations are to appear. One can thus think of sensing the vibrations at the NGS frame-rate and correct for it at the LGS frame-rate with no modification to the real-time computer (RTC) hardware configuration. This novel algorithm, called multi-rate (MR-LQG) follows the initial work of [Raynaud et al., 2008] where a double frame-rate model is proposed to allow for an up-sampled correction. It relies on a continuous-time representation of the disturbances, from which the coarse and fine-grain discrete-time models are built.

2 Sample numerical results

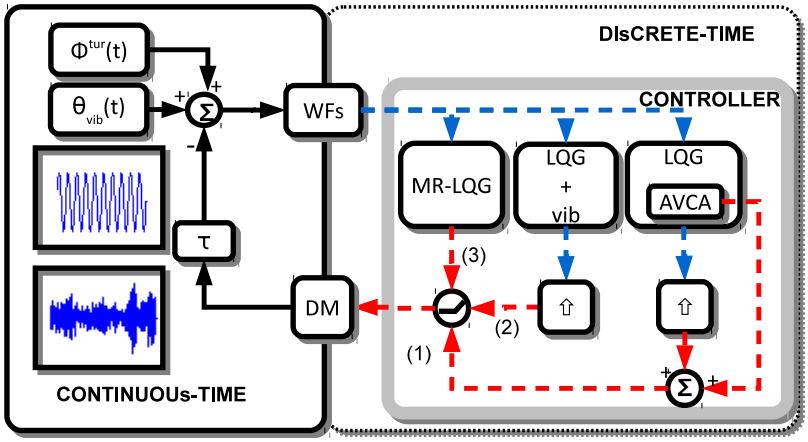

Fig. 1. Closed-loop control architecture of a standard AO system. Straight lines for continuous-time signals and dashed-lines for discrete-time signals (red for f_{max}=800Hz and blue $f_s \leq f_{max}$). The up-sampling blocks (upwards pointing arrows) are *zero-order-hold* blocks. The two windows below θ_{vib} represent a pure-sinusoid and a Gaussian white noise filtered by a 2nd order model (damped vibrations) respectively. Both these disturbances are used as input in the simulations. A constant servo-lag of $\tau = 1$ ms is used to represent real-time computer delays in the loop.

Three controllers were chosen, all sharing a standard LQG controller for atmospheric turbulence rejection with different options for the vibration suppression add-on, following the implementation shown on Fig. 1:

(*i*)-LQG+AVCA : A single-rate LQG controller using in parallel the algorithm of [Lieto et al., 2008] and already studied by [Véran et al., 2010] in the context of NFIRAOS.

(*ii*)-LQG+vib : A single-rate LQG controller with vibration suppression embedded running at the NGS WFS's sampling frequency $f_s = 1/T_s$ using an exactly discretised model for the vibration model proposed in [Correia et al., 2012].

(*iii*)-MR-LQG : A multi-rate LQG controller with vibration suppression embedded running at the NGS WFS's sampling frequency f_s and outputting commands at the maximum frame-rate of f_{max}=800 Hz (of the LGS loop).

Details can be found in [Correia et al., 2012] where a theoretical description is outlined. The simulation parameters are summarised in Table 1.

Table 1. Simulation parameters.

Disturbances	Atmospheric	σ_{TT} = 16.58 mas rms L_0 = 30 m r_0@ 0.5μm = 0.15m
	Wind-shake	σ_{WS} = 7.5 mas rms
	Vibration	σ_{vib} = 18.8 mas rms f_{vib}= 29.5Hz FWHM={0.0274}Hz
WFS	Type	Modal
	Frame-rates	{20, 50, 100, 200, 400, 800}Hz
	Read+dect. noise	{1.1, 11} mas rms
Controllers	LQG	w/ AVCA - CASE (*i*)
	LQG	CASE (*ii*)
	multi-rate LQG	CASE (*iii*)
	disturbance models	order 2
	Servo-lag	1 ms
Mirror	Type	Modal
	Frame-rate	800 Hz
	bandwidth	infinite
Simulation	Duration	45s
	No. modes	1 (tip or tilt)
	wavelength	λ_{WFS}=1.6μm

Figure 2 depicts the performance of the three controllers for a magnitude of $m_v \sim 12$, *i.e* a measurement noise of 1.1 milliarcseconds for vibrations' natural frequencies in the range [2-225] Hz and a peak full width at half-maximum Δf=0.0274Hz. Several comments are in order. First, the bottom-right figure sets the upper limit of the vibration frequency that can be suppressed to be in the range [125-225] Hz, which happens to be roughly 1/4 of the LGS loop frame rate of 800 Hz. Secondly, for vibrations <10Hz the AVCA is ineffective. Divergence at $f_{\text{vib}} = 8$Hz is still to be investigated. In general, the MR-LQG always outperforms all the other algorithms, in particular at low sampling frequencies (see the cyan curve) below the vibration natural frequency.

Figure 3 shows the same results of Fig. 2 for a dim star magnitude resulting in a measurement noise of 11 mas rms. In general the same conclusions apply, but now the difference in performance between the LQG+AVCA and the MR-LQG is not so large, in particular at low sampling frequencies. The same is to say that the measurement error corrupts the measurements in such a way that using the pure-sinusoid model of the AVCA does actually deliver reasonable results with respect to the MR-LQG, despite the system having damped vibrations with FWHM of 0.0274Hz and not a pure sinusoid as the AVCA assumes.

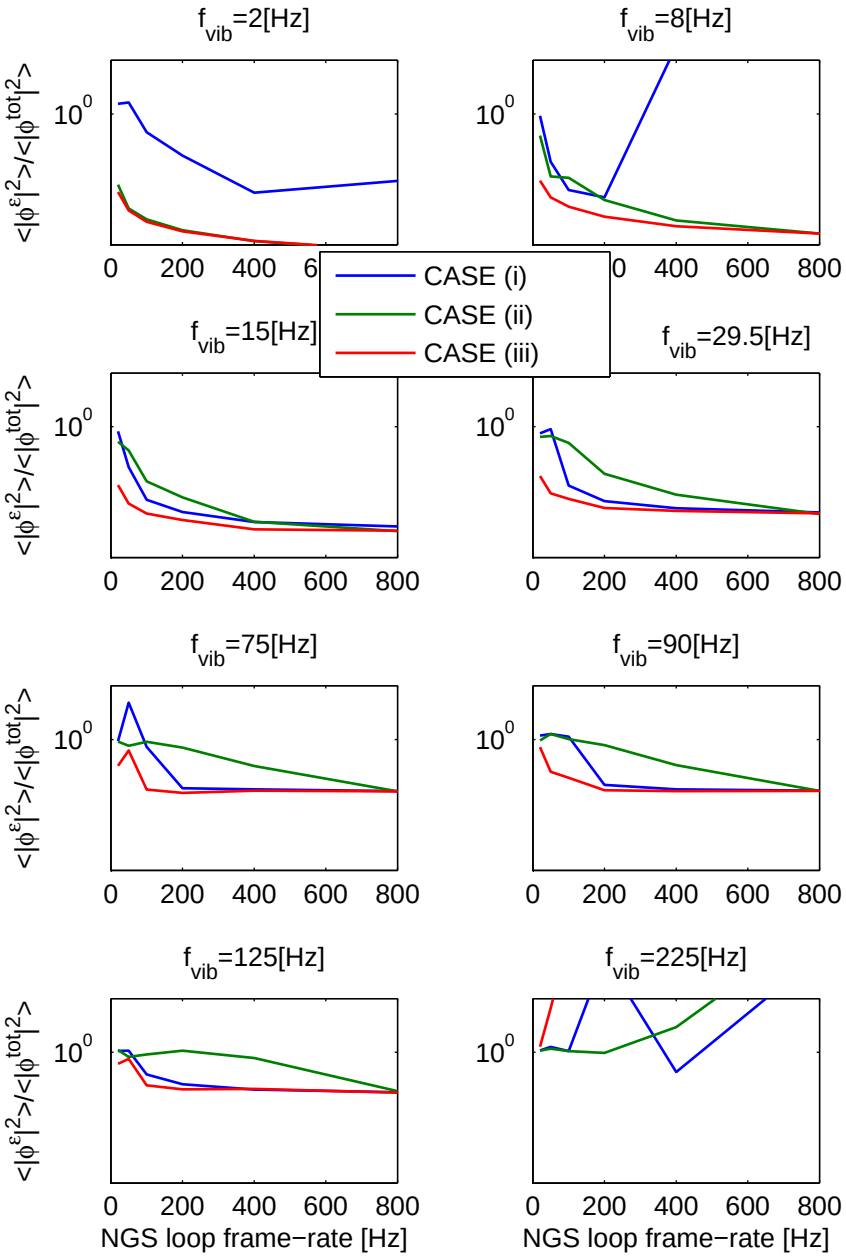

Fig. 2. Measurement noise=1.1mas rms, vibration full width at half-maximum Δf=0.0274Hz. Case (i): LQG+AVCA in blue; case (ii): LQG+single rate vibration suppression in green; case (iii): Multi-rate LQG in red.

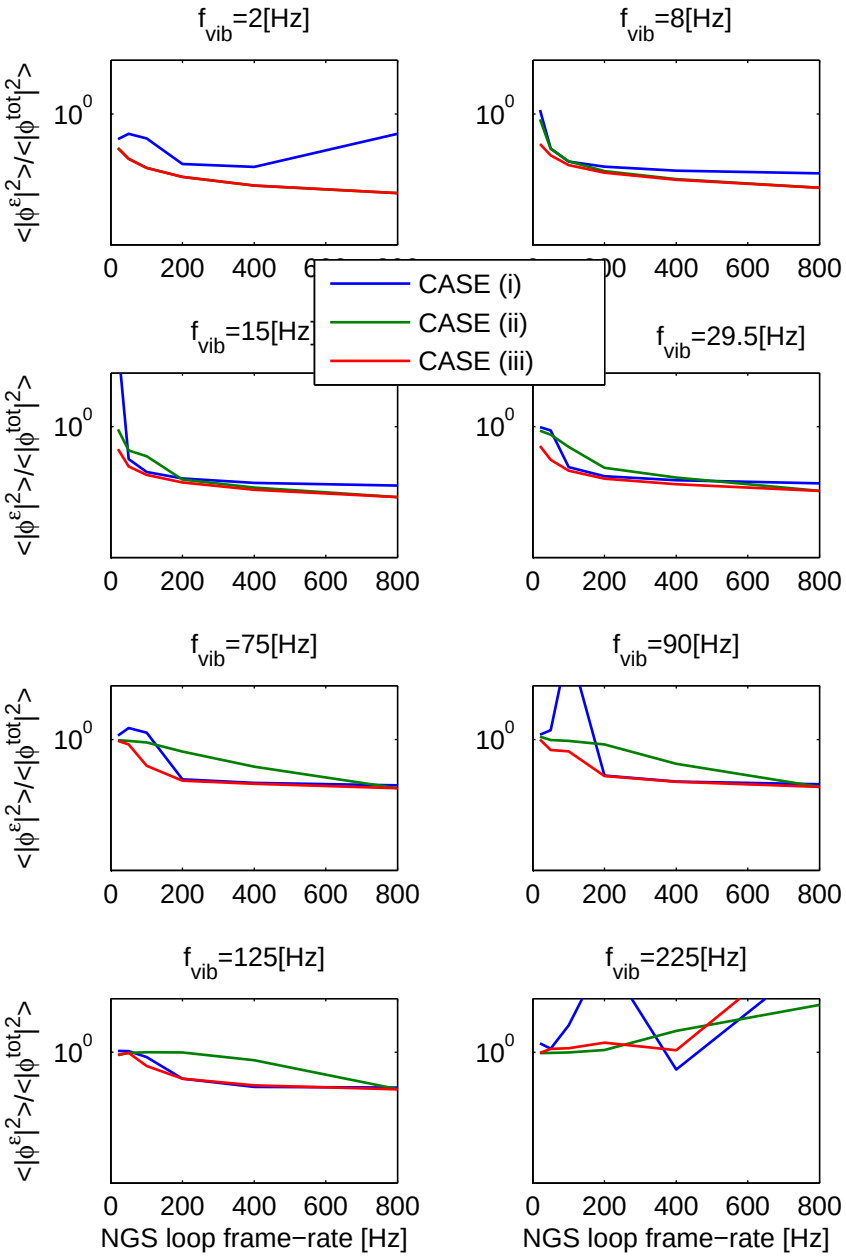

Fig. 3. Performance comparison. Measurement noise=11mas rms, vibration full width at half-maximum Δf=0.0274Hz. Case (i): LQG+AVCA in blue; case (ii): LQG+single rate vibration suppression in green; case (iii): Multi-rate LQG in red.

2.1 Sensitivity to the vibration natural frequency

Another interesting point that has been formulated countless times with respect to the LQG controllers is their stability, in particular when the model and the reality mismatch.

Figure 4 shows a set of 3 plots where the vibration is in this case a pure sinusoid of frequency f_{vib} whereas the model assumes $f_{mod} = f_{\text{vib}} \pm \{0, 2, 5\}\%$. From left to right, the MR-LQG degrades its performance as the mismatch in the vibration central frequency increases. Another striking although expected result from this experiment is that the performance loss is quite less dramatic for the LQG+AVCA, in which case the recursive least-squares of the AVCA is able to correctly track the vibration central frequency adaptively in real-time, providing a higher degree of rejection for this class of vibration signals.

However, as the plots above show, the MR-LQG is better suited for the general-case of damped vibrations, with, as is now seen, the increased stress of correctly identifying the vibrations with a $\sim 2\%$ accuracy, definitely an exacting task. To be totally fair in performing a comparison, the model parameters to be used in the MR-LQG will likewise require an identification procedure that is somewhat similar to the one on the AVCA where such parameters are tracked in real-time during operation. Thus, these results only suggest that the accuracy to be required from the identification is roughly on the order of the percent for the vibration natural frequency.

The same experiment was conducted with damped vibration signals and the same conclusions are reached concerning the accuracy of the identified vibration central frequency.

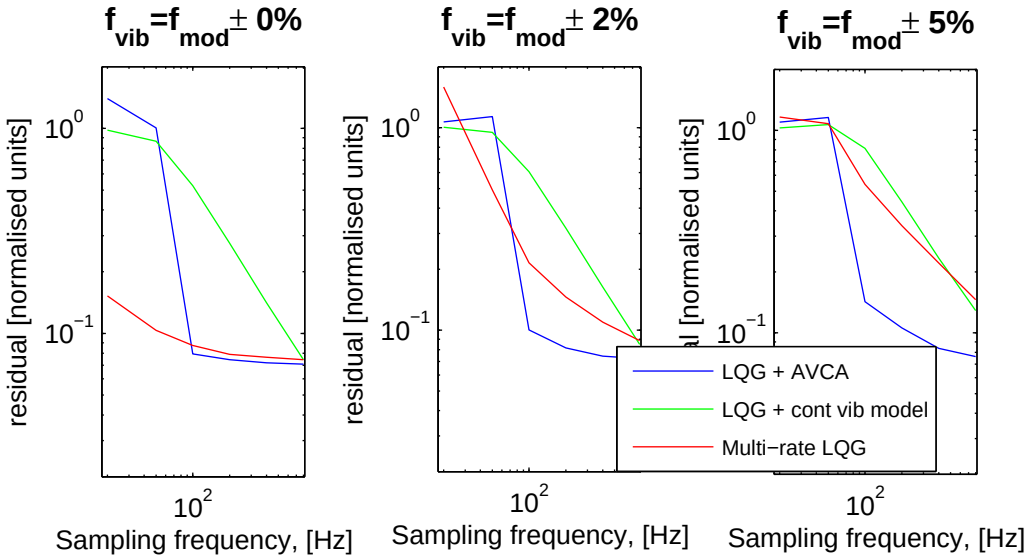

Fig. 4. Sensitivity of algorithms of CASES (i) through (iii) with respect to the model mismatch between the model and the actual vibration central frequency on the system. Measurement noise=1.1mas rms. Case (i): LQG+AVCA in blue; case (ii): LQG+single rate vibration suppression in green; case (iii): Multi-rate LQG in red.

2.2 Outlook

We took a step further in characterising the potential vibration suppression algorithms for NFIRAOS on the TMT.

Numerical results show that vibrations can be suppressed in the range $[2 - 225]$Hz with the upper limit being quite severe in terms of stability stress on the algorithms when using a sampling frame rates within the $[20 - 800]$Hz.

In terms of sensitivity to the vibration central frequency, an accuracy of better than 2% will be required in identifying the model for the MR-LQG to work properly. To this respect, the AVCA algorithm is quite robust in the sense that the suppression signal is continuously adapted in real-time using a recursive least-squares algorithm, making it less exposed to model-system mismatches. This paper now hands over to the identification side of vibrations further developments to check compliance with the conclusions herein.

References

[Borelli et al., 2010] Borelli, J., Trowitzsch, J., Brix, M., Kürster, M., Gässler, W., Bertram, T., and Briegel, F. (2010). The LBT real-time based control software to mitigate and compensate vibrations. In *Proc. of the SPIE*, volume 7740.

[Clenet et al., 2004] Clenet, Y., Kasper, M. E., Ageorges, N., Lidman, C., Fusco, T., Marco, O., Hartung, M., Mouillet, D., Koehler, B., Rousset, G., and Hubin, N. N. (2004). Naco performance: status after 2 years of operation. In Calia, D. B., Ellerbroek, B. L., and Ragazzoni, R., editors, *Proc. of the SPIE*, volume 5490, pages 107–117. SPIE.

[Correia et al., 2011] Correia, C., Veran, J.-P., and Herriot, G. (2011). Advanced vibration suppression algorithms in adaptive optics systems. *J. Opt. Soc. Am. A*.

[Correia et al., 2012] Correia, C., Véran, J.-P., and Herriot, G. (2012). Advanced vibration suppression algorithms in adaptive optics systems. *J. Opt. Soc. Am. A*, 29(3):185–194.

[Hess et al., 2003] Hess, M., Nance, C. E., Vause, J. W., Hrynevych, M., Swain, M. R., and Colavita, M. (2003). Strategy for identifying and mitigating facility vibrations to improve optical performance at the W.M. Keck Observatory. In J. M. Oschmann & L. M. Stepp, editor, *Proc. of the SPIE*, volume 4837, pages 342–351.

[Lieto et al., 2008] Lieto, N. D., Haguenauer, P., Sahlmann, J., and Vasisht, G. (2008). Adaptive vibration cancellation on large telescopes for stellar interferometry. In Schöller, M., Danchi, W. C., and Delplancke, F., editors, *Proc. of the SPIE*, volume 7013, page 70130H. SPIE.

[Meimon et al., 2010] Meimon, S., Petit, C., Fusco, T., and Kulcsar, C. (2010). Tip–tilt disturbance model identification for Kalman-based control scheme: application to XAO and ELT systems. *J. Opt. Soc. Am. A*, 27(11):A122–A132.

[Poyneer and Véran, 2010] Poyneer, L. A. and Véran, J.-P. (2010). Kalman filtering to suppress spurious signals in adaptive optics control. *J. Opt. Soc. Am. A*, 27(11):A223–A234.

[Raynaud et al., 2008] Raynaud, H. F., Kulcsár, C., Correia da Silva, C., and Conan, J.-M. (2008). Multirate LQG AO control. In Hubin, N., Max, C. E., and Wizinowich, P. L., editors, *Proc. of the SPIE*, volume 7015, page 701538. SPIE.

[Véran et al., 2010] Véran, J., Irving, C., Beauvillier, A., and Herriot, G. (2010). Implementation of type-II tip-tilt control in NFIRAOS with woofer-tweeter and vibration cancellation. In *Proc. of the SPIE*, volume 7736.

[Veran and Poyneer, 2009] Veran, J.-P. and Poyneer, L. (2009). Characterization of the T/T conditions at gemini using adaptive optics telemetry data. In Y. Clénet, J.-M. Conan, T. F. and Rousset, G., editors, *1st AO4ELT Conference - Adaptative Optics for Extremely Large Telescopes proceedings*, number 05002. EDP Sciences.

[Wang et al., 2009] Wang, L., Ellerbroek, B., and Veran, J. P. (2009). High fidelity sky coverage analysis via time domain adaptive optics simulations. *Appl. Opt.*, 48(27):5076–5087.